Fine-scale heat flow, shallow heat sources, and decoupled circulation systems at two sea-floor hydrothermal sites, Middle Valley, northern Juan de Fuca Ridge

J. S. Stein
Earth Sciences Department, University of California, Santa Cruz, California 95064
A.T. Fisher
Earth Sciences Department and Institute of Tectonics, University of California, Santa Cruz, California 95064
M. Langseth*
W. Jin
G. Iturrino
Lamont-Doherty Earth Observatory, Palisades, New York 10964
E. Davis
Pacific Geoscience Centre, Geological Survey of Canada, P.O. Box 6000, Sidney, British Columbia V8L 4B2, Canada

ABSTRACT

Fine-scale heat-flow patterns at two areas of active venting in Middle Valley, a sedimented rift on the northern Juan de Fuca Ridge, provide thermal evidence of shallow hydrothermal reservoirs beneath the vent fields. The extreme variability of heat flow is explained by conductive heating immediately adjacent to vents and shallow circulation within sediments above the reservoir. This secondary circulation is hydrologically separated from the deeper system feeding the vents by a shallow conductive lid within the sediments. A similar separation of shallow and deep circulation may also occur at sediment-free ridge-crest hydrothermal environments.

INTRODUCTION

Nearly 25% of the Earth's heat is lost by hydrothermal circulation within the oceanic crust (Lowell et al., 1995), and areas of active, high temperature venting at mid-ocean ridges are important focal points of this cooling. While inferences regarding the subsurface plumbing of these systems have been made on the basis of thermal and chemical data, few data sets provide enough lateral detail to resolve fine-scale, subsurface hydrologic and thermal structures beneath vent fields.

We report results of a fine-scale heat-flow survey of two areas of active venting in Middle Valley, a sedimented rift at the northern end of Juan de Fuca Ridge in the northeast Pacific Ocean (Fig. 1A) (Davis et al., 1992). Because the data were collected at a sufficiently fine scale (20–50 m), the various processes influencing spatial variability in heat flow can be assessed and separated, allowing us to constrain the depth and geometry of hydrothermal reservoirs beneath the vent fields. New data and analyses are consistent with the presence of shallow isothermal zones beneath the vent fields, and provide new insights into the plumbing of ridge-crest hydrothermal systems.

BACKGROUND AND PREVIOUS WORK

Middle Valley has been visited by numerous surface surveys and two Ocean Drilling Program (ODP) expeditions (Davis et al., 1992; Fouquet et al., 1998), that provided information about the lithologic, diagenetic, thermal, and tectonic history of the region. The two primary study sites within Middle Valley are the Dead Dog and Bent Hill hydrothermal fields (Fig. 1).

The Dead Dog vent field (ODP Sites 858 and 1036) is located 6 km west of the normal-faulted eastern edge of Middle Valley and 6 km east of the current valley axis. It is contained within a region of high acoustic backscatter measuring 400 × 800 m (Davis and Villinger, 1992). The vent field hosts at least 20 active chimneys discharging 180 to 276 °C fluids; most vent temperatures are near the high end of this range (Ames et al., 1993; Butterfield et al., 1994). Drilling within the Dead Dog hydrothermal field encountered basaltic basement at 258 m below the sea floor (mbsf) (Davis et al., 1992).

The Bent Hill area (ODP Sites 856 and 1035) is 4 km southeast of the Dead Dog vent field, and 3 km west of the eastern fault scarp of Middle Valley. A single hydrothermal vent, located 500 m south of the topographic high for which the area is named, expels fluid at 265 °C (Ames et al., 1993). A massive sulfide deposit that formed when circulation temperatures were much higher (>350 °C) is located 300 m north of the vent and has been the focus of drilling and coring (Davis and Fisher, 1994).

HEAT-FLOW DATA

More than 550 heat-flow measurements had previously been made in Middle Valley (Davis and Villinger, 1992); however, these data were relatively widely spaced, and navigational uncertainties made it difficult to assess accurately the extent and character of individual vent areas. We measured 266 and 125 thermal gradients at Dead Dog and Bent Hill hydrothermal areas, respectively. These measurements were positioned with real-time, differential, Global Positioning System navigation and sea-floor transponders, and provided location uncertainties of ≤5–10 m. We used 2.5- and 3.5-m-long, 11-thermistor, violin-bow heat-flow probes, as well as autonomous outrigger thermistors attached to piston- and gravity-core barrels, to map the distribution of heat flow around the vent fields. Equilibrium thermal gradients for each penetration were determined using a modified version of the method described by Villinger and Davis (1987). Heat flow was calculated from site-specific thermal conductivity-depth functions determined from more than 1000 needle-probe thermal conductivity measurements made on recovered cores.

At the Dead Dog area, heat-flow values range from 0.65 to 50 W/m^2 and form a bullseye pattern, with the highest spatial gradients coinciding with the acoustic edge of the vent field. Within the field, the pattern is complex, with both high and low values found near active vents. At the Bent Hill area, heat-flow values range from 0.23 to 28 W/m^2, and all values above 10 W/m^2 are located within 75 m of the single active vent. A zone of elevated heat flow also surrounds the massive sulfide deposit (Fisher et al., 1997).

*Deceased.

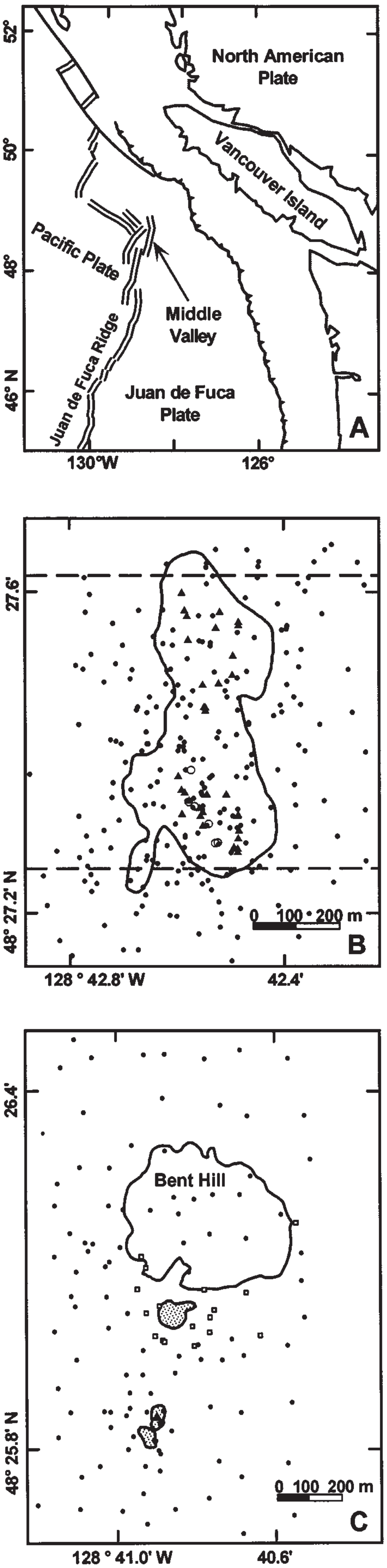

Figure 1. A: Tectonic map showing northern Juan de Fuca Ridge and Middle Valley. B: Dead Dog hydrothermal area. Outline of area of high acoustic backscatter (Davis and Villinger, 1992) (solid line) shown with heat-flow measurements (solid circles) and vent locations (solid triangles). Open circles show locations of diffuse flow recognized from curved thermal gradients or elevated temperatures above sea floor. Data inside the east-west swath between dashed lines are plotted in Figure 2A. C: Bent Hill hydrothermal area. Stippled areas are sulfide deposits. Middle deposit contains single active vent (solid triangle). Heat-flow measurements are divided into two categories: those elevated above conductive, shallow source model by refraction (open squares) and those that are not (solid circles).

HYDROLOGIC INTERPRETATION OF THERMAL OBSERVATIONS

We interpret the distribution of heat flow at the two sites in terms of several superimposed processes that locally elevate or depress heat flow relative to regional "background" values. The background heat flow represents a balance between large-scale magmatic heat supply and conductive and hydrothermal heat loss. Locally, the heat flow is determined by the thickness of the relatively impermeable sediments overlying a more permeable "hydrologic basement" aquifer, and is 400–600 mW/m^2 within several kilometers surrounding the two sites (Davis and Villinger, 1992; Fisher et al., 1997). Heat-flow values consistently elevated above this mean near the vent areas are the consequence of locally shallow hydrologic basement, a conductive contribution from vents, and secondary convection within shallow sediments. This last process is also responsible for heat-flow values within the vent areas that are very close to, or even below, regional background values. In the remainder of this paper, we consider these heat-flow patterns and their implications for the hydrogeology of the vent fields.

An analytical, conductive model (Hardee and Larson, 1980) was used to evaluate the thermal effect of a shallow hydrothermal reservoir below each vent field. The model allows calculation of the steady-state, one-dimensional heat flow at the sea floor away from the edges of a buried, isothermal body. The body is assumed to have a flat top, vertical sides, and to extend to infinite depth. We assume that this body represents a hydrothermal reservoir where hot, vigorously circulating water maintains essentially isothermal conditions and provides a heat and fluid source for the vent field. Heat flow at the surface above this source is approximated as:

$$u_s = \frac{z_s}{\pi}\left[2\left(\frac{q_m}{q_s}\right) + \ln\left(\frac{1-\left(\frac{q_m}{q_s}\right)}{1+\left(\frac{q_m}{q_s}\right)}\right)\right], \qquad (1)$$

where u_s is the horizontal distance from the vertical edge of the source, z_s is the depth to the top of the source, q_m is the measured heat flow value, and q_s is the heat flow immediately above the source. This value, referred to as the "mean vent-field heat flow," is fixed by the depth to the top of the source, the thermal conductivity of the overlying sediments, and the constant-temperature boundary conditions of the source and the sea floor. This is the highest heat flow that can be explained by this part of our conceptual model, and heat flow decreases with increasing distance from the source edge.

We assume that the source is at 280 °C. This assumption is based on maximum observed vent temperatures (Butterfield et al., 1994), thermal data collected in shallow sediments and open boreholes during drilling (Davis et al., 1992; Langseth and Becker, 1994), and alteration products that lack evidence for higher temperatures associated with the present phase of venting (Ames et al., 1993; Davis and Fisher, 1994). The remaining free parameters in this model are the depth to the top of the source, the location of the source edges, and the background heat flow.

To compare model results with observations, we projected heat flow data onto a series of profiles across the vent fields. Two example profiles are shown in Figure 2, along with several applications of the model. For each assumed source depth, model curves were shifted by varying background heat flow and edge location, with the goal of matching the lateral gradient of the highest values outside the vent field, as well as the average of values within the vent field. We do not attempt to explain the scatter of values within the vent field with this model, nor the occurrence of values below the conductive prediction. This variability can be explained with additional processes, as described later.

Around the Dead Dog vent field, the data are most consistent with a model comprising a source depth of 30 mbsf, an edge location coincident with the acoustic boundary of the vent field, and a background heat flow of 390 to 440 mW/m^2. Using the observed thermal conductivity profile within shallow sediments (Davis et al., 1992), this corresponds to a mean vent field heat flow of 10.6 W/m^2, a value near the mean of all heat-flow measurements made within the vent field and in good agreement with drilling measurements and other conductive models (Davis et al., 1992; Davis and Fisher, 1994). A shallower source depth would elevate the mean vent field value well above all but a few extreme observations (Fig. 2A). A greater source depth would explain fewer measurements outside the vent field because the source would become correspondingly wider.

Application of this model to the Bent Hill vent area yields a source depth of 150 mbsf, a source width of 200 m north to south, and background heat flow of 390 to 430 mW/m^2. The model is less-well constrained in the Bent Hill area because of sparser data coverage and complications associated with three additional contributions to the sea-floor heat-flow distribution (Fig. 2B): refraction through thermally conductive massive and disseminated sulfide (Davis et al., 1992; Fouquet et al., 1998), a small topographic effect that lowers heat flow on top of Bent Hill, and conductive heating immediately adjacent to the active vent.

The conductive contribution to sea-floor heat flow associated with discrete venting, q_{cv}, can be approximated by considering a vent as an isothermal pipe rising vertically from depth (Sleep and Wolery, 1978):

$$q_{cv} = \frac{4kT_v}{\pi u_v \ln\left(\frac{z_v}{\pi r_v}\right)}, \qquad (2)$$

where k is the thermal conductivity, r_v is vent radius, z_v is depth to the base of the vent, T_v is the vent temperature, and u_v is distance from the vent at the sea floor. Calculations using equation 2 and parameters appropriate for these sites indicate that heat flow falls rapidly within a few tens of meters of the vent orifice (Fig. 2B). This model explains some of the highest values measured in both vent areas, particularly several measurements close to the single Bent Hill vent, but it cannot explain conductive trends hundreds of meters from vents.

The final process we consider for explaining the observed heat-flow patterns is diffuse flow of pore fluids through shallow sediments. Evidence for diffuse upflow within the Dead Dog vent field includes several measurements of essentially isothermal conditions within the shallow sediments; instances where the heat-flow probe failed to penetrate the sea floor, but temperatures measured by the thermistors indicated that warm water was rising around the fallen lance; and earlier submersible observations (Ames et al., 1993). The rise of warm pore fluids through sediments will increase heat flow close to the sea floor (Bredehoeft and Papadopoulos, 1965; Sleep and Wolery, 1978). Seepage fluxes in excess of about 30 cm/yr are readily detectable within shallow sediments from upward curvature in thermal gradients beyond that explained by reasonable variations in thermal conductivity. Few thermal gradients display curvature characteristic of fluid flow out of the sea floor, indicating that regions of significant upward seepage are spatially isolated.

There are also several indications of shallow fluid recharge within the vent fields. Measurements using in situ pore-pressure instruments in the shallow subsurface of the Dead Dog vent area demonstrate that these sediments have negative pore-pressure gradients (–0.4 to –0.1 kPa/m)

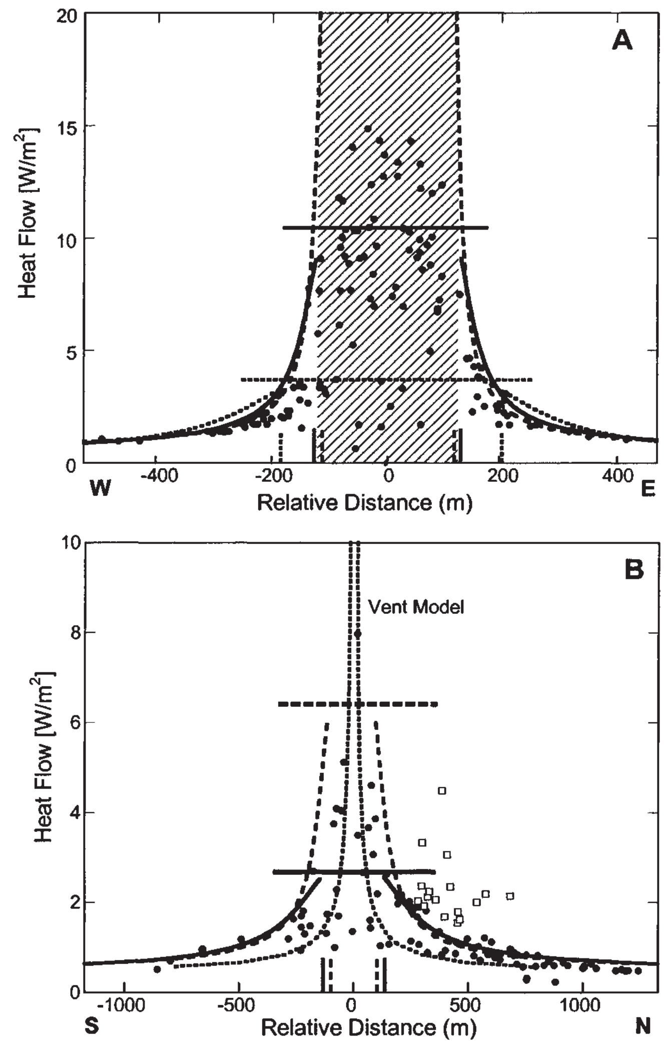

Figure 2. A: West-east profile of heat flow across Dead Dog vent field. Data (solid circles) are from within swath shown in Figure 1B and are projected onto west-east profile. Hachured region represents area inside acoustic backscatter boundary. Three isothermal source models are shown: top of source at 10 mbsf (dashed curve), 30 mbsf (solid curve), and 100 mbsf (dotted curve). Horizontal lines represent mean vent field heat flow for respective models, 29.8 W/m^2 (off scale and not shown), 10.6 W/m^2, and 3.8 W/m^2, respectively. Short vertical lines along x-axis indicate modeled edges of heat source. B: South-north profile of all heat-flow values across Bent Hill site except for highest values adjacent to vent (off scale). Two isothermal models, top of source at 50 mbsf (dashed curve) and 150 mbsf (solid curve), are shown. Mean vent field heat flow for isothermal source models are 6.7 W/m^2 and 2.8 W/m^2, respectively. Pipe model (equation 2) shown (dotted line) is for a 280 °C pipe of radius 1 m extending 200 mbsf in a medium with thermal conductivity 1 W/m per °C. Locations of high heat flow in northern half of profile (open squares, Fig. 1C) cluster around high thermal conductivity sulfide deposit and base of Bent Hill.

(Langseth et al., 1996; Schultheiss, 1997; Fouquet et al., 1998). Shallow subsurface alteration patterns in the Dead Dog vent field indicate seawater reacting with the sediments (Ames et al., 1993; Davis et al., 1992). Because curvature of a thermal gradient induced by downward flow is difficult to identify with short heat-flow probes, drawdown of cold seawater would often result in thermal gradients that are depressed below those predicted by the isothermal source model, but that appear conductive near the sea floor.

Local fluid recharge must be part of a secondary convection system that is decoupled from the deep circulation system supplying active vents, because the primary (deep) hydrothermal system below Dead Dog vent field is greatly overpressured relative to hydrostatic (+180 kPa, Hole 858G [Davis and Becker, 1998]), not underpressured like the shallow sediments. In addition, vent fluid chemistry reflects little seawater-sediment reaction at high temperatures (Butterfield et al., 1994), hence the recharge-discharge cycle through the sediments must be shallow.

Secondary circulation within the shallow sediments of the vent fields is thermally driven by a combination of a shallow, relatively isothermal reservoir and subvertical vent conduits. Free convection in a homogeneous, isotropic 30-m-thick layer heated from below requires a permeability on the order of 10^{-14} m^2, based on Rayleigh number considerations; however, subcritical convection would occur where there are heterogeneities in permeability, thermal structure, or both. Pore-fluid underpressures would accompany lateral circulation within shallow sediments. Underpressures consistent with measurements in the Dead Dog vent field (Langseth et al., 1996; Schultheiss, 1997) in combination with laboratory measurements of sediment permeability (Fisher et al., 1994), give a downward seepage flux of 30 cm/yr, great enough to reduce shallow thermal gradients by 50%.

DISCUSSION AND CONCLUSIONS

The modeled source depths at Dead Dog and Bent Hill vent fields (30 mbsf and 150 mbsf, respectively) coincide with lithologic and geochemical horizons identified by drilling. Shallow sediment alteration below the Dead Dog area increases rapidly with depth (Fouquet et al., 1998), and an indurated layer encountered at 30 mbsf was hypothesized to be a hydrothermal cap rock (Davis et al., 1992; Davis and Fisher, 1994). In these systems, chlorinity is higher in the vent fluids than in bottom water and is essentially a conservative tracer. Chlorinity profiles from several holes in the Dead Dog vent field indicate lateral flow of seawater within the upper 30 mbsf, while below this depth pore fluids have a vent-fluid signature. (Davis et al., 1992; Fouquet et al., 1998). At the Bent Hill vent field, indurated layers were cored and identified as sulfide feeder zones containing mineralized sediments, including highly silicified layers at about 170 and 190 mbsf (Fouquet et al., 1998). Chlorinity profiles just west of the main sulfide deposit exhibit a clear excursion toward vent fluid chemistry below 150 mbsf (Fouquet et al., 1998).

The formation of a shallow reaction zone within the sedimentary section may have resulted from the focusing of heat and solutes up through the top of the now-buried volcanic edifice underlying the Dead Dog vent field. Alteration, lithification, and fracturing of sediments (Davis and Becker, 1994) would have occurred after (or as) they were deposited on the previously exposed (Langseth and Becker, 1994) basement high, and would result in the formation of a thin, conductive boundary layer between underlying (deep, high temperature) and overlying (shallow, low temperature) hydrothermal systems. Alternatively, the high thermal gradients and vigorous mixing of cold seawater and hot hydrothermal fluids may result in rapid mineral precipitation, dynamically maintaining a low-permeability alteration front. Below this barrier to flow, high fluid pressures can hydrofracture and enhance permeability within the sediments, helping to maintain the vigorous circulation and sustaining isothermal conditions in the deeper system (Davis et al., 1992). The diagenetic, hydrologic, and thermal boundary layer is pierced below high-temperature vents to allow localized discharge, but recharge to this main system must occur well outside the vent fields.

This conceptual model may shed light on bare-rock hydrothermal systems at ridge crests, although the lack of a low-permeability sediment blanket is likely to result in a deeper reaction zone. The methodology used in this study is suitable for bare-rock ridge-crest environments, provided that the spatial differences in heat flow can be resolved at the sea floor. Newly developed heat-flow instrumentation for sediment-free sea-floor environments (Johnson and Hutnak, 1997) provides hope that this may soon be possible.

ACKNOWLEDGMENTS

This research was supported by National Science Foundation grants OCE 95-96253 and OCE 95-28438. Mark Person and an anonymous reviewer helped improve this manuscript.

REFERENCES CITED

Ames, D. E., Franklin, J. M., and Hannington, M. D., 1993, Mineralogy and geochemistry of active and inactive chimneys and massive sulfide, Middle Valley, northern Juan de Fuca Ridge: An evolving hydrothermal system: Canadian Mineralogist, v. 31, p. 997–1024.

Bredehoeft, J. D., and Papadopoulos, I. S., 1965, Rates of vertical groundwater movement estimated from the Earth's thermal profile: Water Resources Research, v. 1, p. 325–328.

Butterfield, D. A., McDuff, R. E., Franklin, J., and Wheat, C. G., 1994, Geochemistry of hydrothermal vent fluids from Middle Valley, Juan de Fuca Ridge, *in* Mottl, M. J., Davis, E. E., Fisher, A. T., and Slack, J. F., eds., Proceedings of the Ocean Drilling Program, Scientific results, Volume 139: College Station, Texas, Ocean Drilling Program, p. 395–410.

Davis, E. E., and Villinger, H., 1992, Tectonic and thermal structure of the Middle Valley sedimented rift, northern Juan de Fuca Ridge, *in* Davis, E. E., Mottl, M. J., Fisher, A. T., et al., Proceedings of the Ocean Drilling Program, Initial reports, Volume 139: College Station, Texas, Ocean Drilling Program, p. 9–41.

Davis, E. E., and Becker, K., 1994, Formation temperature and pressures in a sedimented rift hydrothermal system: 10 months of CORK observations, Holes 857D and 858G, *in* Mottl, M. J., Davis, E. E., Fisher, A. T., and Slack, J. F., eds., Proceedings of the Ocean Drilling Program, Scientific results, Volume 139: College Station, Texas, Ocean Drilling Program, p. 649–666.

Davis, E. E., and Fisher, A. T., 1994, On the nature and consequences of hydrothermal circulation in the Middle Valley sedimented rift: Inferences from geophysical and geochemical observations, Leg 139, *in* Mottl, M. J., Davis, E. E., Fisher, A. T., and Slack, J. F., eds., Proceedings of the Ocean Drilling Program, Scientific results, Volume 139: College Station, Texas, Ocean Drilling Program, p. 695–717.

Davis, E. E., and Becker, K., 1998, Borehole observatories record driving forces for hydrothermal circulation in young oceanic crust: Eos (Transactions, American Geophysical Union), v. 79, p. 165–170.

Davis, E. E., Mottl, M. J., Fisher, A. T., et al., 1992, Proceedings of the Ocean Drilling Program, Initial reports, Volume 139: College Station, Texas, Ocean Drilling Program, 1026 p.

Fisher, A. T., Fischer, K., Lavoie, D., Langseth, M., and Xu, J., 1994, Geotechnical and hydrological properties of sediments from Middle Valley, northern, Juan de Fuca Ridge, *in* Mottl, M. J., Davis, E. E., Fisher, A. T., and Slack, J. F., eds., Proceedings of the Ocean Drilling Program, Scientific results, Volume 139: College Station, Texas, Ocean Drilling Program, p. 627–647.

Fisher, A., Langseth, M., Baker, P., Ryan, W., Stein, J., Glenn, S., Shultheiss, P., Zierenberg, R., Iturrino, G., Jin, W., Darlington, E., Goodfellow, W., Daniel, D. N., Conly, A., Cross, S., Grove, M., and Cramer, B., 1997, The devil's in the details: Fine-scale hydrogeology of areas of active venting in Middle Valley, northern Juan de Fuca Ridge: Eos (Transactions, American Geophysical Union), v. 78, p. 165–170.

Fouquet, Y., Zierenberg, R. A., and Miller, D. J., 1998, Proceedings of the Ocean Drilling Program, Initial reports, Volume 169: College Station, Texas, Ocean Drilling Program, 592 p.

Hardee, H. C., and Larson, D. W., 1980, Thermal techniques for characterizing magma body geometries: Geothermics, v. 9, p. 237–249.

Johnson, H. P., and Hutnak, M., 1997, Conductive heat loss in recent eruptions at mid-ocean ridges: Geophysical Research Letters, v. 24, p. 3089–3092.

Langseth, M., and Becker, K., 1994, Structure of igneous basement at sites 857 and 858 based on Leg 139 downhole logging, *in* Mottl, M. J., Davis, E. E., Fisher, A. T., and Slack, J. F., eds., Proceedings of the Ocean Drilling Program, Scientific results, Volume 139: College Station, Texas, Ocean Drilling Program, p. 573–583.

Langseth, M. G., Schultheiss, P., Fisher, A. T., and Ryan, W. B. F., 1996, Local recharge in an area of active hydrothermal venting: Pore pressure gradient measurements over a sedimented ridge axis in Middle Valley, Juan de Fuca Ridge: Eos (Transactions, American Geophysical Union), v. 77, p. S257.

Lowell, R. P., Rona, P. A., and Von Herzen, R. P., 1995, Seafloor hydrothermal systems: Journal of Geophysical Research, v. 100, p. 327–352.

Schultheiss, P., 1997, Advances in fluid flow determinations for marine hydrogeology using pore pressure measurements: Eos (Transactions, American Geophysical Union), v. 78, p. 672.

Sleep, N. H., and Wolery, T. J., 1978, Egress of hot water from midocean ridge hydrothermal systems: Some thermal constraints: Journal of Geophysical Research, v. 83, p. 5913–5922.

Villinger, H., and Davis, E. E., 1987, A new reduction algorithm for marine heat flow measurements: Journal of Geophysical Research, v. 92, p. 12846–12856.

Manuscript received April 14, 1998
Revised manuscript received August 26, 1998
Manuscript accepted September 4, 1998